Absence of Substrate Channeling between Active Sites in the *Agrobacterium tumefaciens* IspDF and IspE Enzymes of the Methyl Erythritol Phosphate Pathway†

Christian Lherbet,‡ Florence Pojer,§ Stéphane B. Richard,§ Joseph P. Noel,§ and C. D. Poulter*,‡

Department of Chemistry, University of Utah, Salt Lake City, Utah 84112, and Howard Hughes Medical Institute, The Jack H. Skirball Center for Chemical Biology and Proteomics, The Salk Institute for Biological Studies, La Jolla, California 92037

Received October 3, 2005; Revised Manuscript Received December 7, 2005

ABSTRACT: The conversion of 2-*C*-methyl-D-erythritol 4-phosphate (MEP) to 2-*C*-methyl-D-erythritol 2,4-cyclodiphosphate (cMEDP) in the MEP entry into the isoprenoid biosynthetic pathway occurs in three consecutive steps catalyzed by the IspD, IspE, and IspF enzymes, respectively. In *Agrobacterium tumefaciens* the *ispD* and *ispF* genes are fused to encode a bifunctional enzyme that catalyzes the first (synthesis of 4-diphosphocytidyl-2-*C*-methyl D-erythritol) and third (synthesis of 2-*C*-methyl-D-erythritol 2,4-cyclodiphosphate) steps. Sedimentation velocity experiments indicate that the bifunctional IspDF enzyme and the IspE protein associate in solution, raising the possibility of substrate channeling among the active sites in these two proteins. Kinetic evidence for substrate channeling was sought by measuring the time courses for product formation during incubations of MEP, CTP, and ATP with the IspDF and IspE proteins with and without an excess of the inactive IspE(D152A) mutant in the presence or absence of 30% (v/v) glycerol. The time dependencies indicate that the enzyme-generated intermediates are not transferred from the IspD active site in IspDF to the active site of IspE or from the active site in IspE to the active site of the IspF module of IspDF.

Isopentenyl diphosphate (IPP)[1] and dimethylallyl diphosphate (DMAPP) are the two five-carbon building blocks used in nature to construct the hydrocarbon skeletons of isoprenoid compounds (*1*). IPP and DMAPP are synthesized by two different biosynthetic pathways: the mevalonate (MVA) pathway (*2*) found in mammals, plants, fungi, and Gram-positive bacteria and the 2-*C*-methyl-D-erythritol 4-phosphate (MEP) pathway found in algae, cyanobacteria, eubacteria, apicomplexan parasites, and plant chloroplasts (*3*).

The MEP biosynthetic pathway (*4*) is outlined in Scheme 1. Three central steps are required to convert MEP into 2-*C*-methyl-D-erythritol 2,4-cyclodiphosphate (cMEDP), a methylerythritol derivative containing a unique cyclic diphosphate moiety. Methylerythritol 4-phosphate cytidylyltransferase, encoded by *ispD*, condenses MEP with cytosine 5′-triphosphate (CTP) to give 4-diphosphocytidyl-2-*C*-methyl-D-erythritol (CDP-ME) and inorganic pyrophosphate (PP_i) (*5*). CDP-ME kinase encoded by *ispE* catalyzes an ATP-dependent phosphorylation of CDP-ME to produce 4-diphosphocytidyl-2-*C*-methyl-D-erythritol 2-phosphate (CDP-MEP) (*6*, *7*). Finally, CDP-MEP is converted to cMEDP with concomitant release of CMP by methylerythritol 2,4-cyclodiphosphate synthase, encoded by *ispF* (*8*). In most organisms, *ispD* and *ispF* are encoded by separate genes. However, bioinformatic analysis of deposited genomic data revealed 14 different instances in which i*spD* and *ispF* are fused genes resulting

Scheme 1: MEP Pathway for Biosynthesis of Isoprenoid Compounds

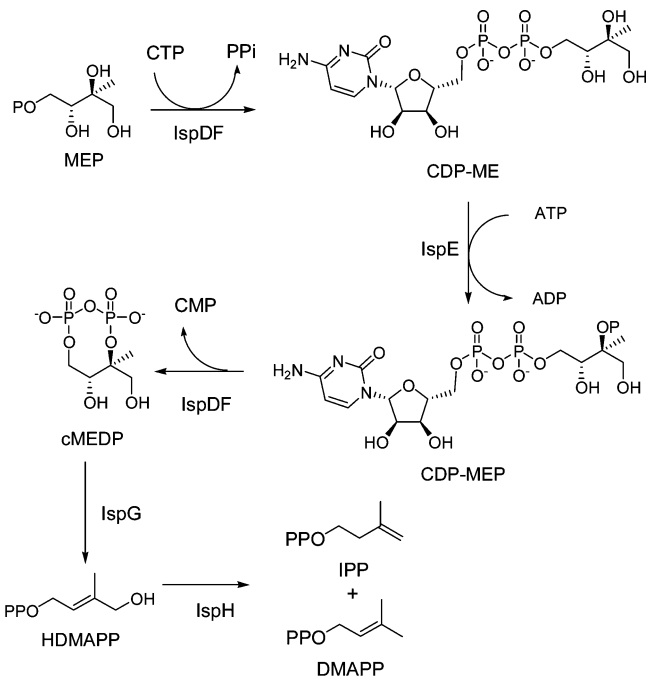

† Supported by NIH Grants GM21328 (C.D.P.) and AI51438 (J.P.N.) and by a postdoctoral fellowship from the Deutsche Forschungsgemeinschaft (F.P.).

* To whom correspondence should be addressed. E-mail: poulter@chem.utah.edu. Phone: 801-581-6685. Fax: 801-581-4391.

‡ University of Utah.

§ The Salk Institute for Biological Studies.

[1] Abbreviations: Amp, ampicillin; ATP, adenosine 5′-triphosphate; CTP, cytosine 5′-triphosphate; CDP-ME, 4-diphosphocytidyl-2-*C*-methyl-D-erythritol; CDP-MEP, 4-diphosphocytidyl-2-*C*-methyl-D-erythritol 2-phosphate; cMEDP, 2-*C*-methyl-D-erythritol 2,4-cyclodiphosphate; DMAPP, dimethylallyl diphosphate; HDMAPP, 4-hydroxydimethylallyl diphosphate; IPP, isopentenyl diphosphate; IPTG, isopropyl 1-thio-*β*-D-galactopyranoside; MEP, 2-*C*-methyl-D-erythritol 4-phosphate; MVA, mevalonate; PMSF, phenylmethanesulfonyl fluoride; SDS−PAGE, sodium dodecyl sulfate−polyacrylamide gel electrophoresis.

10.1021/bi0520075 CCC: $33.50
Published on Web 02/22/2006

Table 1: Oligonucleotides Used in This Study

enzyme	oligonucleotide	sequence
IspDF	CL0610DFC58sen	5′AAAGCCCATATGCAGGAAAGTACTATGAAATTCGGCATCGTCATC3′
	CL0610DFC58ant	5′AAAGCCGGATCCATTATAGCGGTCTGCCTTGGTAGACGACGGTG3′
IspE	CL0429EC58sen	5′AAAAGCCCATATGCGCCTGCATGAGGTTTCCGGGGC3′
	CL0429EC58ant	5′AAAGCCGGATCCATTAAATGGTCCGCGTTGCGTGAAAATACCAGC3′
IspE(D152A)	AMAISPE007	5′GAAACTGGGCGCGGCTGTACCGATGTGC3′
	GC-AMAISPE007	5′GCACATCGGTACAGCCGCGCCCAGTTTC3′

in the production of a single bifunctional polypeptide possessing both IspD and IspF activity (*9*−*11*). Biochemical analysis confirms that the bifunctional enzyme catalyzes the first and third steps in the conversion of MEP to cMEDP.

This unusual arrangement of enzymes within a metabolic pathway could potentially enhance flux through the MEP pathway by direct metabolite channeling in a putative IspDF/IspE complex. Although no evidence for protein−protein interactions among the individual IspD, IspE, and IspF proteins from *Escherichia coli* has been presented, the IspDF fusion protein and the IspE protein from *Campylobacter jejuni* and *Agrobacterium tumefaciens* are reported to associate (*11*). We now report kinetic studies that address the issue of metabolite channeling in the *A. tumefaciens* enzymes.

EXPERIMENTAL PROCEDURES

Materials. Restriction enzymes were purchased from New England Biolabs. KlenTaq-LA DNA polymerase mix was purchased from Sigma. Ni-NTA resin was from Qiagen. MEP was obtained from Echelon Biosciences, Inc. IPTG was from USB. ATP and CTP were obtained from Sigma. [γ-^{32}P]-ATP and [α-^{32}P]CTP were from NEN. All other chemicals were purchased from Sigma-Aldrich. TLC plates (Polygram Sil N-HR) were purchased from Macherey & Nagel. ImageQuant 5.2 (Molecular Dynamics) was used to quantify the radioactivity on TLC plates.

Cloning. PCR amplification of *A. tumefaciens IspDF* from genomic DNA (ATCC 33970D) was performed with primers CL0610DFC58sen and CL0610DFC58ant and Klen Taq polymerase according to the following procedure: 94 °C (3 min) and 61 °C (2 min) for 1 cycle, followed by 68 °C (2 min), 94 °C (45 s), and 61 °C (45 s) for 30 cycles (Table 1). The PCR product was purified using the GFX gel band purification kit and ligated into pGEM-Teasy with T4 ligase (Promega). The resulting plasmid was transformed into JM109 cells, and positive colonies were detected by blue/white screening in the presence of IPTG and X-Gal. Constructs possessing the correct insert were chosen on the basis of restriction digests with *Nde*I and *Bam*HI and were confirmed by automated DNA sequencing (University of Utah Core Facility). The *Nde*I/*Bam*H1 insert was subcloned into the *Nde*I and *Bam*HI sites of pET15b, resulting in an expression clone containing an N-terminal His_6 tag sequence. The desired construct, pET15b/*At*DF, was used to transform electrocompetent XL1-blue cells. Positive constructs based upon restriction enzyme analysis with *Nde*I and *Bam*HI were sequenced.

IspE was obtained by PCR amplification using primers CL0429EC58sen and CL0429EC58ant and *A. tumefaciens* genomic DNA (ATCC33970D) using the following PCR settings: 94 °C (2 min) and 61 °C (2 min) for 1 cycle, followed by 68 °C (2 min), 94 °C (30 s), and 61 °C (30 s) for 30 cycles. The *IspE* expression clone was obtained using a procedure similar to that described above for *IspDF*.

The *IspE*(D152A) site-directed mutant was obtained using the QuickChange kit from Stratagene. The mutated gene was amplified using primers AMAISPE007 and GC-AMAISPE007 (Table 1) to give pET15b/*At*E(D158A), which was then sequenced to verify the mutation.

Expression of IspDF, IspE, and IspE(D152A) and Protein Purification. BL21(DE3)pLysS was transformed with pET15b/*At*DF, pET15b/*At*E, and pET15b/*At*E(D152A), and 5 mL LB cultures (100 μg/mL ampicillin) of the transformants were grown overnight at 37 °C, with shaking. Four cultures (two for each enzyme), each containing 1 L of LB and 100 μg/mL ampicillin, were inoculated with 2 mL of the overnight culture and were grown at 37 °C, with shaking at 250 rpm, until $OD_{600} = 0.6$. IPTG was then added to 1 mM (final concentration), incubation was continued for 5.5 h, and cells were harvested by centrifugation and stored at −80 °C.

Cell paste was resuspended in 50 mM sodium phosphate, pH = 8.0, 300 mM NaCl, and 10 mM imidazole (lysis buffer). Complete protease inhibitor cocktail tablets (Roche) and lysozyme (1 mg/mL) were added, the cells were lysed by sonication, cellular debris was removed by centrifugation, and the His-tagged enzymes were purified by chromatography on Ni-NTA agarose (Qiagen).

$CaCl_2$ (2.5 mM final concentration) was added to the solutions of His_6-tagged IspDF, IspE, and IspE(D152A), each containing a thrombin cleavage site. Thrombin (50 units) was added to 6 mg of each protein in elution buffer (50 mM sodium phosphate, pH = 8.0, 300 mM NaCl, 250 mM imidazole) at 4 °C. After 12 h, thrombin was removed by adding benzamidine−agarose (Sigma). The samples were filtered and diluted with the lysis buffer to reduce the imidazole concentration below 100 mM. Finally, Ni-NTA resin was added, and unproteolyzed proteins and the His_6 fragment were removed by Ni-NTA chromatography. The flow-through fractions were concentrated with a Centriprep-10 unit (Centricon) and dialyzed against 0.1 mM Tris-HCl, pH 7.6 (measured at 37 °C), using a 10000 molecular weight cutoff dialysis cassette (Pierce). The protein concentrations were determined by the Bradford method (*12*).

Analytical Ultracentrifugation. Sedimentation velocity experiments were performed using a Beckman XL-1 analytical ultracentrifugation with absorbance optical detection. Three different concentrations of purified wild-type IspE and IspE(D152A) in 25 mM HEPES, pH 7.5, and 100 mM NaCl were used for sedimentation studies. Protein samples were centrifuged at a rotor speed (An50 Ti) of 42000 rpm, and absorbance data at 280 nm were collected. Analyses of the sedimentation velocity data were performed using the program SEDFIT (*13*).

Enzyme-Generated Products. Enzymatic reactions were carried out at 37 °C in 0.1 mM Tris-HCl buffer, pH 7.6, containing 5 mM DTT, 10 mM $MgCl_2$, 150 μM CTP, 150 μM ATP, 500 μM racemic MEP, 0.24 μM IspDF, 0.31 μM IspE, and varying concentrations (0, 0.3, 0.6, 1.4, 3.1, 6.3, 12.5 μM) of IspE(D152A) in a final volume of 50 μL. [^{32}P]-NTPs were diluted from 5 mM stock solutions of 40 μCi/μmol CTP and 320 μCi/μmol ATP. In control experiments, samples were preincubated for 5 and 20 min, respectively, in the presence of all substrates, except for radiolabeled ATP and CTP, or enzyme. Reactions were initiated by addition of CTP. After 15 min, the reactions were quenched with 50 μL of methanol and were put on ice. TLC analysis (Polygram Sil N-HR; Macherey & Nagel) was performed by spotting 3.5 μL of the reaction mixture and developing the plates with 1-propanol/ethyl acetate/H_2O (6:1:3 v/v/v). Radioactivity was quantified with a Molecular Dynamics Typhoon 8600 phosphorimager.

Time Course Studies. A solution of 500 μM MEP (racemic), 0.24 μM IspDF, and 0.31 μM IspE in 0.1 M Tris-HCl buffer, pH 7.6 (37 °C), containing 5 mM DTT, in a final volume of 150 μL was preincubated for 10 min at 37 °C. ATP (150 μM) and [γ-^{32}P]CTP (150 μM, 320 μCi/μmol) were added sequentially to initiate the reaction. At various times, 6 μL portions of the mixture were removed and quenched with 6 μL of methanol. After 61 min, additional 0.5 μg portions of each enzyme were added to the reaction mixture. Identical reactions were run in the presence of 3.1 μM IspE or a mixture of 3.1 μM IspE and 31 μM IspE-(D152A). After 61 min, 0.5 μg of IspDF and 0.5 μg of IspE were added to the reaction mixtures. The reactions were repeated in 0.1 M Tris-HCl buffer containing 30% (v/v) glycerol at pH 7.6 (37 °C) with 3.12 μM IspE or 3.12 μM IspE and 31 μM IspE(D152A). After 61 min, 0.5 μg of IspDF and 0.5 μg of IspE were added to the reaction mixtures.

RESULTS

Expression of IspDF, IspE, and IspE(D152A) and Protein Purification. A. tumefaciens IspDF and IspE were amplified by PCR and cloned into pET15b. Expression of the genes in *E. coli* BL21(DE3) cells provided His_6-tagged proteins that were easily purified by chelation chromatography on Ni-NTA resin, resulting in protein judged to be >95% pure based upon SDS−PAGE analysis. The His_6 tags were removed with thrombin digestion and repurification over benzamidine−Sepharose and addition Ni-NTA resin.

An inactive mutant of *A. tumefaciens* IspE was obtained by replacing the catalytically essential Asp152 with Ala. D152 is located in a conserved LGADVP motif found in the *A. tumefaciens* and *E. coli* proteins. Analysis of the X-ray structure of *E. coli* IspE suggests that the aspartate acts as a general base to deprotonate the *tert*-hydroxyl group of CDP-ME during its phosphorylation by ATP (*14*). The mutant gene was cloned into pET15b, and the His_6-tagged protein was purified as described above. The N-terminal His_6 tag preceding a thrombin protease cleavage site was removed, and the nontagged protein was used as is in subsequent experiments.

Analytical Ultracentrifugation of IspE and IspE(D152A). Sedimentation velocity experiments were carried out to accurately measure the oligomerization state of mutant and wild-type IspE. The sedimentation coefficient (*s*) of both IspE proteins at different concentrations is identical (~2.1 S) and is consistent with a monomeric state for this small molecule kinase assuming a globular conformation. The sedimentation experiments indicated that wild-type IspE and the D152A mutant exist as monomers (99%) in equilibrium with ~1% of an undetermined form (Figure 1). These observations are consistent with data in the literature (*11*). These results demonstrate that the D152A mutation does not substantially alter the overall conformation of the protein relative to wild-type IspE.

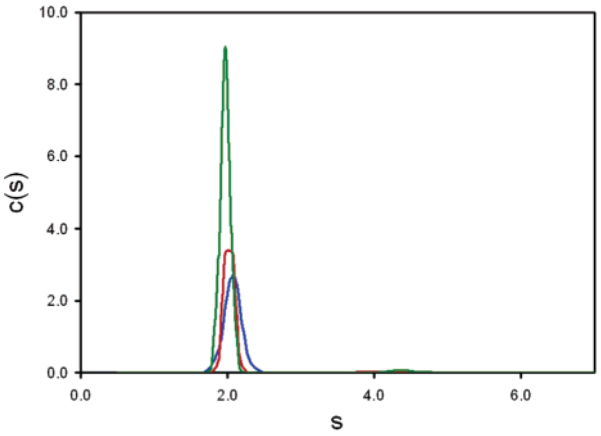

FIGURE 1: Sedimentation velocity experiments performed with 25 μM wild-type IspE (blue), 28 μM IspE(D152A) (red), and 50 μM IspE(D152A) (green).

Effect of the IspE(D152A) Mutant on the Conversion of MEP to cMEDP by Wild-Type Enzymes. First, IspE(D152A) was checked for activity by incubating the purified enzyme with MEP, CTP, ATP, and wild-type IspDF under the standard conditions for product formation and analysis. Formation of cMEDP was not detected at IspE(D152A) concentrations up to 300 μM (data not shown). Assuming a detection limit of at least 20% for cMEDP in the product mixture, we estimate that the D152A mutant is at least 10000 times less active than wild-type IspE. This loss of activity is consistent with the proposal that D152 acts as a general base required for deprotonation and subsequent phosphorylation of the *tert*-hydroxyl group of CDP-ME (*14*).

Radiolabeled ATP and CTP were used to monitor the formation of CDP-ME, CDP-MEP, CMP, and cMEDP. As illustrated in Figure 2, addition of IspE(D152A) during the 15 min preincubation of a mixture of MEP, [α-^{32}P]CTP, and [γ-^{32}P]ATP, IspDF, and wild-type IspE did not alter the product distribution at IspE(D152A)/IspE ratios >40:1. Varying the preincubation time prior to initiating the assay did not alter the distribution of products.

Time Course for Formation of Products in the Presence and Absence of IspE(D152A). Following the protocol described above, the time course for conversion of MEP to cMEDP using IspDF and IspE was monitored by TLC (Figure 3). The intermediates and final product, CDP-MEP, CDP-ME, CMP, and cMEDP, were resolved and quantified by phosphorimaging (*9*). Plots of the concentrations of the intermediates and the final product cMEDP are shown in Figure 4. For the experiment illustrated in Figure 4A, the concentrations of IspDF and IspE were chosen so that MEP was rapidly converted to CDP-ME, followed by a slower conversion of CDP-ME to CDP-MEP. Radioactivity from

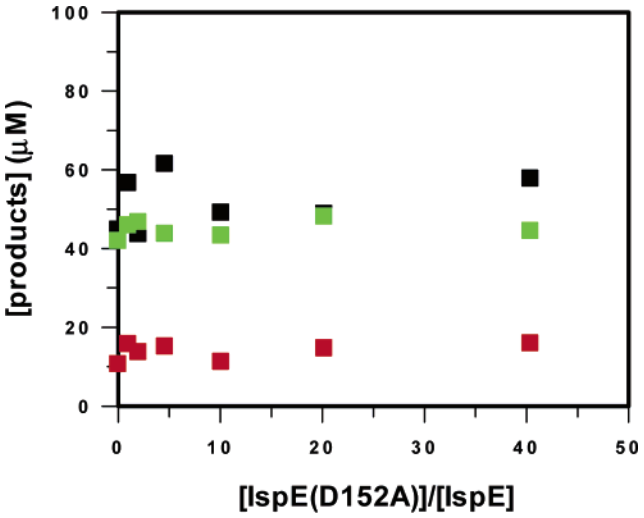

FIGURE 2: Product distributions for *A. tumefaciens* IspDF and IspE with added IspE(D152A): CDP-ME (black boxes), CDP-MEP (red boxes), CMP or cMEDP (green boxes). Substrate and enzyme concentrations were as follows: 150 μM CTP (40 μCi/μmol), 150 μM ATP (320 μCi/μmol), 500 μM MEP (racemic), 0.24 μM IspDF, 0.31 μM IspE, and different concentrations (0, 0.3, 0.6, 1.4, 3.1, 6.3, 12.5 μM) of IspE(D152A) in a final volume of 50 μL.

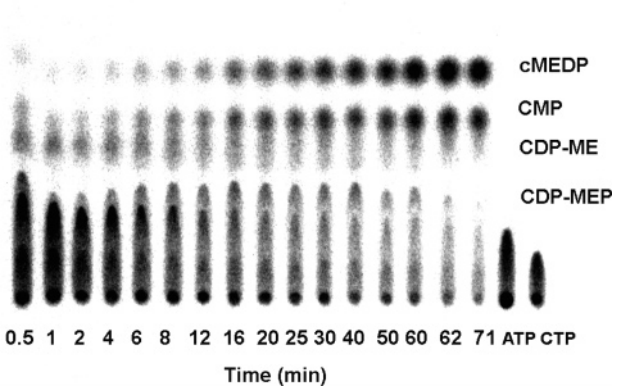

FIGURE 3: TLC plate showing the time course for the formation of CDP-ME, CDP-MEP, CMP, cMEDP catalyzed by IspDF (0.24 μM), and IspE (0.31 μM). At 61 min an additional 0.5 μg portion of each enzyme was added. ATP and CTP lanes represent blank controls without enzyme.

CMP, or a degradation product that accumulated with time, tailed into the spot for CDP-ME, which interfered with our ability to accurately measure the CDP-ME concentration after ~10 min. The concentration of CDP-MEP reached a maximum after ~15 min and never accumulated to levels above 15% of the total. The concentration of IspE was increased 10-fold for the time course shown in Figure 4B. In this case, the concentration of CDP-MEP reached a maximum of ~30 μM (corresponding to approximately 20% of the total) within 5 min and slowly decreased as the reactions proceeded. These results indicate that the relative catalytic efficiency of the IspF subunit is high and that the limiting step is the formation of CDP-MEP even when the IspE protein in present in a 13-fold molar excess. Figure 4C shows a time course for the same substrate and enzyme concentrations used in Figure 4B, except for the addition of a 10-fold molar excess of the inactive IspE(D152A) mutant relative to wild-type IspE. For the time course shown in Figure 4A, the concentrations of CDP-ME, CMP, and cMEDP are essentially equal after ~12 min. When the

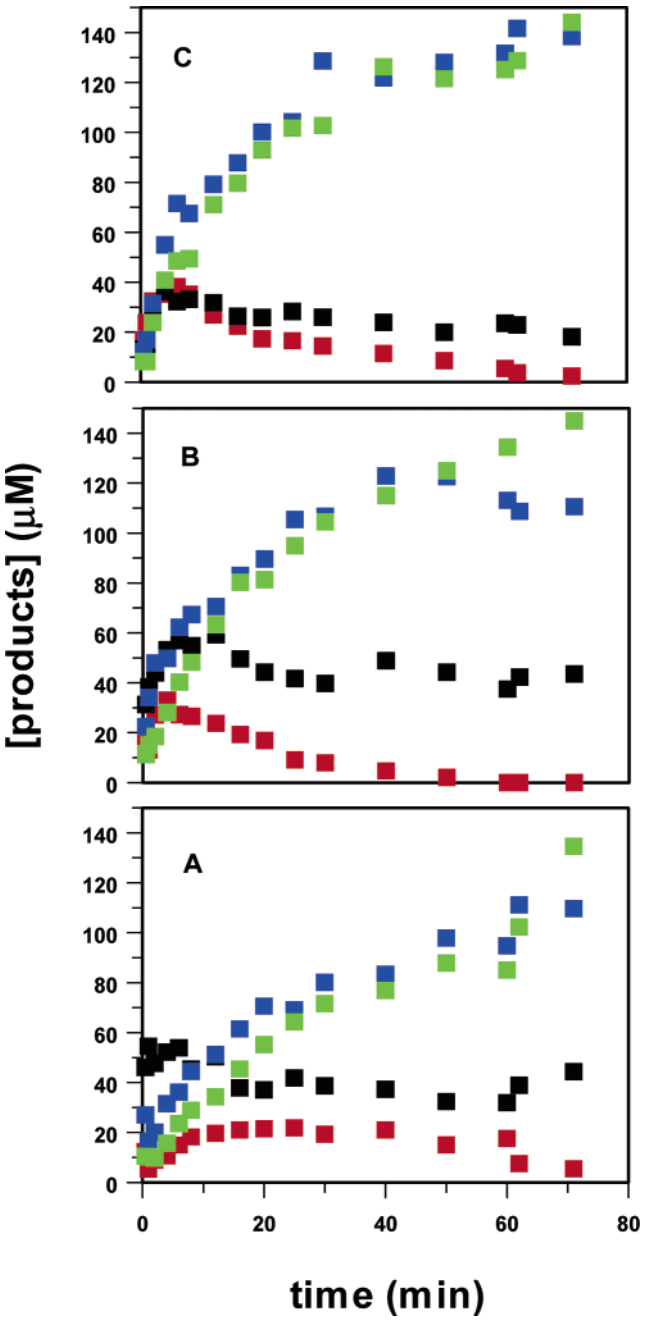

FIGURE 4: Time courses for the formation of CDP-ME + side product (black boxes), CDP-MEP (red boxes), CMP (blue boxes), and cMEDP (green boxes). Panel A: IspDF (0.24 μM) and IspE (0.31 μM). Panel B: IspDF (0.24 μM) and IspE (3.1 μM). Panel C: IspDF (0.24 μM), IspE (3.1 μM), and IspE(D152A) (31.2 μM).

concentration of IspE is increased 10-fold, this equivalency time point drops to ~4 min and is essentially unchanged (Figure 4B). Addition of excess IspE(152A) protein does not substantially alter the time course (Figure 4C). At longer reaction times the "apparent" concentration of CDP-ME levels off while those of the other intermediates decrease. We attribute this to an unidentified product that slowly accumulated during the incubation and migrates between CDP-ME and CMP. A comparison of the overall time courses shown in panels A and B of Figure 4 reveals that IspE(D152A) does not significantly alter the flux from MEP through CDP-ME and CDP-MEP, consecutively, resulting in cMEDP. The time course experiments with 3.1 μM IspE were repeated in assay buffers containing 30% (v/v) glycerol

in the presence and the absence of the IspE(D152A) mutant (*15*). The increased viscosity of the medium due to glycerol did not noticeably alter the time course of the reaction (see Supporting Information). These kinetic results, focused on the metabolic flux through a reconstituted pathway of three MEP pathway enzymes, strongly argue against enhanced flux due to substrate channeling between the *A. tumefaciens* IspDF and IspE proteins or to the formation of higher local concentrations of intermediates produced in a multienzyme complex.

DISCUSSION

The bifunctional IspDF enzymes catalyze two nonconsecutive reactions in the MEP pathway, MEP to CDP-ME and CDP-MEP to cMEDP, respectively. The intermediate step, CDP-ME to CDP-MEP, is catalyzed by the ATP-dependent IspE kinase. Sedimentation velocity studies indicate that the IspDF and IspE enzymes from *A. tumefaciens* and *C. jejuni* associate in solution to form complexes consisting of up to 18 catalytic centers (*11*). No evidence was presented for an 18 catalytic center complex formed by association of the IspD, IspE, and IspF proteins from *E. coli* (*11*). These observations are consistent with a hypothesis that enhanced metabolic flux in the MEP pathway at least from MEP to cMEDP may result either by reducing the distance over which reactive intermediates must diffuse as they move from one active site to another or by providing for direct substrate channeling among the active sites of a preassembled complex of IspDF and IspE (*11*).

The formation of multiprotein complexes of biosynthetic enzymes comprising metabolic pathways offers an attractive and powerful mechanism for enhancing the efficiency and flux of moving intermediates through a pathway. Perhaps the most impressive examples of such efficiency and flux are found in polyketide biosynthesis where a combination of multifunctional enzymes and multiprotein complexes permit tethered intermediates to be efficiently shuttled from one active site to the next as an extraordinarily complex set of molecules is assembled (*16*−*18*). Several methods have been developed to study substrate channeling between two enzymes (*19*, *20*), including competition experiments that employ a wild-type enzyme and a large excess of an inactive mutant that can replace the active enzyme in the multienzyme complex. In our experiments, addition of a 10-fold excess of the inactive IspE(D152A) mutant did not alter the time course for three reactions, MEP to CDP-ME to CDP-MEP to cMEDP in the middle portion of the MEP pathway of isoprenoid biosynthesis.

The observable flux through a pathway might also increase due to an increase in the local concentration of intermediates when the enzymes are in close proximity (*19*). Depending on the structure of the complex, this effect can be enhanced by an increase in the viscosity of the medium (*15*, *21*). Our results demonstrate that increasing the viscosity of the medium by adding the microviscogen glycerol does not affect the time course of the consecutive reactions in the presence or absence of IspE(D152A). If the flux from MEP to CDP-ME, then to CDP-MEP, and finally to cMEDP was enhanced by direct substrate channeling or by an increase in the "local" concentrations of the intermediates due to the close proximity of the active sites in the complex, incorporation of the inactive mutant should measurably decrease the kinetic efficiency of the biosynthetic steps in question (*22*).

Does the fusion of the *IspD* and *IspF* genes, in concert with the association of the IspDF and IspE proteins, constitute a complex that facilitates the conversion of MEP to cMEDP? Under the conditions tested by our experiments, facilitation of metabolite transfer and production does not occur. Neither of these scenarios was observed.

There are other examples of bifunctional enzymes which do not channel substrates, for example, the GlmU protein (*23*) and phosphoribosyl-anthranilate isomerase-indoleglycerol-phosphate synthase (*24*). Even in a case where channeling was "leaky" in a three-reactant system and the proximity of the newly released intermediate increased the probability of it productively reaching the next active site in the pathway (*25*), the presence of high concentrations of an inactive mutant for the second step should alter the flux through the three steps. The absence of experimental evidence for an enhancement of metabolic flux through the reactions catalyzed by the IspDF/IspE complex raises the question of what possible utility the IspDF fusion or formation of an IspDF/IspE complex serves in the host cell. At this point, the metabolic logic behind the gene fusion remains unclear and may be related to a yet undiscovered regulatory role in the MEP pathway.

SUPPORTING INFORMATION AVAILABLE

Radiochromatograms of TLC plates for the experiments described in Figures 2 and 4 and radiochromatograms as well as graphs for time course experiments in 30% (v/v) glycerol. This material is available free of charge via the Internet at http://pubs.acs.org.

REFERENCES

1. Bochar, D. A., Freisen, J. A., Stauffacher, C. V., and Rodwell, V. W. (1999) in *Comprehensive Natural Products Chemistry* (Cane, D., Ed.) Vol. 2, pp 15−44, Pergamon Press, Oxford.
2. Rohmer, M. (1999) The discovery of a mevalonate-independent pathway for isoprenoid biosynthesis in bacteria, algae and higher plants, *Nat. Prod. Rep. 16*, 565−574.
3. Eisenreich, W., Schwarz, M., Cartayrade, A., Arigoni, D., Zenk, M. H., and Bacher, A. (1998) The deoxyxylulose phosphate pathway of terpenoid biosynthesis in plants and microorganisms, *Chem. Biol. 5*, R221−R233.
4. Eisenreich, W., Rohdich, F., and Bacher, A. (2001) Deoxyxylulose phosphate pathway to terpenoids, *Trends Plant Sci. 6*, 78−84.
5. Rohdich, F., Wungsintaweekul, J., Fellermeier, M., Sagner, S., Herz, S., Kis, K., Eisenreich, W., Bacher, A., and Zenk, M. H. (1999) Cytidine 5′-triphosphate-dependent biosynthesis of isoprenoids: YgbP protein of *Escherichia coli* catalyzes the formation of 4-diphosphocytidyl-2-*C*-methylerythritol, *Proc. Natl. Acad. Sci. U.S.A. 96*, 11758−11763.
6. Kuzuyama, T., Takagi, M., Kaneda, K., Dairi, T., and Seto, H. (2000) Formation of 4-(cytidine 5′-diphospho)-2-*C*-methyl-D-erythritol from 2-*C*-methyl-D-erythritol 4-phosphate by 2-*C*-methyl-D-erythritol 4-phosphate cytidylyltransferase, *Tetrahedron Lett. 41*, 703−706.
7. Luttgen, H., Rohdich, F., Herz, S., Wungsintaweekul, J., Hecht, S., Schuhr, C. A., Fellermeier, M., Sagner, S., Zenk, M. H., Bacher, A., and Eisenreich, W. (2000) Biosynthesis of terpenoids: YchB protein of *Escherichia coli* phosphorylates the 2-hydroxy group of 4-diphosphocytidyl-2-*C*-methyl-D-erythritol, *Proc. Natl. Acad. Sci. U.S.A. 97*, 1062−1067.
8. Herz, S., Wungsintaweekul, J., Schuhr, C. A., Hecht, S., Lüttgen, H., Sagner, S., Fellermeier, M., Eisenreich, W., Zenk, M. H., Bacher, A., and Rohdich, F. (2000) Biosynthesis of terpenoids: YgbB protein converts 4-diphosphocytidyl-2-*C*-methyl-D-erythritol

2-phosphate to 2-*C*-methyl-D-erythritol 2,4-cyclodiphosphate, *Proc. Natl. Acad. Sci. U.S.A. 97*, 2486-2490.
9. Testa, C. A., Lherbet, C., Pojer, F., Noel, J. P., and Poulter, C. D. (2006) Cloning and expression of IspDF from *Mesorhizobium loti*. Characterization of a bifunctional protein that catalyzes nonconsecutive steps in the methylerythritol pathway, *Biochim. Biophys. Acta* (in press).
10. Gabrielsen, M., Rohdich, F., Eisenreich, W., Grawert, T., Hecht, S., Bacher, A., and Hunter, W. N. (2004) Biosynthesis of isoprenoids: a bifunctional IspDF enzyme from *Campylobacter jejuni*, *Eur. J. Biochem. 271*, 3028−3035.
11. Gabrielsen, M., Bond, C. S., Hallyburton, I., Hecht, S., Bacher, A., Eisenreich, W., Rohdich, F., and Hunter, W. N. (2004) Hexameric assembly of the bifunctional methylerythritol 2,4-cyclodiphosphate synthase and protein−protein associations in the deoxy-xylulose-dependent pathway of isoprenoid precursor biosynthesis, *J. Biol. Chem. 279*, 52753−52761.
12. Bradford, M. M. (1976) A rapid and sensitive method for the quantitation of microgram quantities of protein utilizing the principle of protein-dye binding, *Anal. Biochem. 72*, 248−254.
13. Dam, J., and Schuck, P. (2005) Sedimentation velocity analysis of heterogeneous protein-protein interactions: Sedimentation coefficient distributions c(s) and asymptotic boundary profiles from Gilbert-Jenkins theory, *Biophys. J. 89*, 651−666.
14. Miallau, L., Alphey, M. S., Kemp, L. E., Leonard, G. A., McSweeney, S. M., Hecht, S., Bacher, A., Eisenreich, W., Rohdich, F., and Hunter, W. N. (2003) Biosynthesis of isoprenoids: crystal structure of 4-diphosphocytidyl-2-*C*-methyl-D-erythritol kinase, *Proc. Natl. Acad. Sci. U.S.A. 100*, 9173−9178.
15. Otsuki, T., Mori, M., and Tatibana, M. (1982) Studies on channeling of carbamoyl-phosphate in the multienzyme complex that initiates pyrimidine biosynthesis in rat ascites hepatoma cells, *J. Biochem. 92*, 1431−1437.
16. Beck, B. J., Aldrich, C. C., Fecik, R. A., Reynolds, K. A., and Sherman, D. H. (2003) Substrate recognition and channeling of monomodules from the pikromycin polyketide synthase, *J. Am. Chem. Soc. 125*, 12551−12557.
17. Hartung, I. V., Rude, M. A., Schnarr, N. A., Hunziker, D., and Khosla, C. (2005) Stereochemical assignment of intermediates in the rifamycin biosynthetic pathway by precursor-directed biosynthesis, *J. Am. Chem. Soc. 127*, 11202−11203.
18. Admiraal, S. J., Khosla, C., and Walsh, C. T. (2005) A switch for the transfer of substrate between nonribosomal peptide and polyketide modules of the rifamycin synthetase assembly line, *J. Am. Chem. Soc. 127*, 13664−13665.
19. Geck, M. K., and Kirsch, J. F. (1999) A novel, definitive test for substrate channeling illustrated with the aspartate aminotransferase/malate dehydrogenase system, *Biochemistry 38*, 8032−8037.
20. Anderson, K. S. (1999) Fundamental mechanisms of substrate channeling, *Methods Enzymol. 308*, 111−145.
21. Morgunov, I., and Srere, P. A. (1998) Interaction between citrate synthase and malate dehydrogenase. Substrate channeling of oxaloacetate, *J. Biol. Chem. 273*, 29540−29544.
22. Nogaj, L. A., and Beale, S. I. (2005) Physical and kinetic interactions between glutamyl-tRNA reductase and glutamate-1-semialdehyde aminotransferase of *Chlamydomonas reinhardtii*, *J. Biol. Chem. 280*, 24301−24307.
23. Gehring, A. M., Lees, W. J., Mindiola, D. J., Walsh, C. T., and Brown, E. D. (1996) Acetyltransfer precedes uridylyltransfer in the formation of UDP-*N*-acetylglucosamine in separable active sites of the bifunctional GlmU protein of *Escherichia coli*, *Biochemistry 35*, 579−585.
24. Eberhard, M., Tsai-Pflugfelder, M., Bolewska, K., Hommel, U., and Kirschner, K. (1995) Indoleglycerol phosphate synthase-phosphoribosyl anthranilate isomerase: comparison of the bifunctional enzyme from *Escherichia coli* with engineered monofunctional domains, *Biochemistry 34*, 5419−5428.
25. Kis, K., and Bacher, A. (1995) Substrate channeling in the lumazine synthase/riboflavin synthase complex of *Bacillus subtilis*, *J. Biol. Chem. 270*, 16788−16795.

BI0520075